Predicting the Yield Stress of Geomaterials from Their Microstructure

Lesueur, Martin; Zhang, Xinrui; Poulet, Thomas; Veveakis, Manolis

DOI
10.1007/978-3-031-22213-9_21

Publication date
2023

Document Version
Final published version

Published in
Multiscale Processes of Instability, Deformation and Fracturing in Geomaterials - Proceedings of 12th International Workshop on Bifurcation and Degradation in Geomechanics

Predicting the Yield Stress of Geomaterials from Their Microstructure

Martin Lesueur[1(✉)], Xinrui Zhang[1], Thomas Poulet[2], and Manolis Veveakis[3]

[1] Delft University of Technology, Delft, Netherlands
m.lesueur@tudelft.nl
[2] CSIRO Mineral Resources, Perth, Australia
[3] Duke University, Durham, USA

Abstract. The seminal work of Gurson (J Eng Mater Technol 99:2–5, 1977) on a simplified pore structure, a single spherical pore, first provided a theoretical relationship between the yield stress and the porosity. This contribution extends the approach to determine the macroscopic yield of a porous material by taking explicitly into account its internal structure. As the yielding of a porous material is controlled by the geometry of its internal structure, we postulate that it is nearly independent of the constitutive plastic behaviour of the material. Here, we show that the influence of that internal structure on the yield could be retrieved from a finite element computation with just an elastoplastic ideal (J2) material equivalent of the skeleton's. With some basic knowledge about the skeleton's mechanical properties, this process allows the determination of the yield stress without requiring the experimental compression of the material. We showcase the predictive power of the method against experimental testing, initially for a unit cell following Gurson, i.e., unique cylindrical void in a 3D printed cylinder sample. Eventually, the applicability of the method is demonstrated on a complex 3D printed rock microstructure, reconstructed from a sandpack's CT-scan.

Keywords: Yield stress · 3D printing · Microstructure

1 Introduction

Many studies are aiming at accounting for the micro-structural influence on rock mechanical properties, whether on elastic properties [9, 15], rock strength [3, 6, 7, 10], or plastic flow law [6, 7], to cite only a few. This contribution focuses on the yield value, as necessary step to model a rock's behaviour past its limit of elasticity. Some models already account for the impact of microstructure on yield through the simplest parameter describing that microstructure: porosity [5–8]. In this contribution, we look at the microstructure from a more general perspective.

The only unambiguous determination of mechanical yield point is possibly restricted to the simplest case of ideal non-porous linear elastic and ideally plastic materials, such as metals for instance. Indeed, experimental compression tests of such materials lead to

E. Pasternak and A. Dyskin (Eds.): IWBDG 2022, 2023.
https://doi.org/10.1007/978-3-031-22213-9_21

characteristic stress-strain curves displaying a sharp transition between the linear elasticity and ideal plasticity. For more complex materials, however, including real geomaterials like porous rocks, a homogenisation procedure is necessary.

A convenient starting point to study the links between microstructure and yield is to consider the theoretical scenario of the simplest configuration, which consists of a single spherical pore, following the seminal work from [7]. To avoid any non-essential complexity and restrict the study to the influence of microstructure, he selected a rigid and ideally plastic material. The outer geometry of the unit cell was taken as spherical, like the void shape, in order to retain the geometrical isotropy and benefit from the symmetry in the analysis. Using the upper-bound limit analysis method, Gurson obtained an approximate upper solution to the yield surface of the hollow sphere geometry, which proved to be precise enough to fit experimental data [18, 20]. Numerous studies followed, extending his work and improving on the model. These include derivations accounting for other shapes of voids (e.g. elliptical [5]), the interaction between voids [4, 19], or the consideration of more complex matrix materials (e.g. viscoplasticity [1]).

By taking an ideally plastic material, the constitutive relationships extracted can indeed be solely attributed to the microstructure, i.e. without any interfering influence of other material properties. Gurson's analysis was an important first step towards our understanding of the influence of the microstructure. We aim now at verifying how the information gathered above holds for physical materials, by complementing our theoretical analysis with an equivalent experimental study on a real material. We verify that the yield of a porous material is equal to that of a virtual porous material with an equivalent ideal elasto-plastic skeleton, instead of considering its more realistic plastic behaviour (including rheology). Additionally, we propose to extend Gurson's type of analysis from limit load to macroscopic yield, measured on stress-strain curves with an energetic method, following Lesueur et al. [14].

The material selected in this contribution is 3D printed polylactic acid (PLA), whose mechanical response from laboratory experiments is plotted and modelled in Fig. 1. 3D printing presents great advantages for the experimental validation of our approach. The 3D printing technique allows a perfect control of the samples' internal structure, whose influence we are characterising. In addition, the printed material has a very reproducible behaviour, as observed by the superposition of curves in Fig. 1. 3D printed PLA is particularly well-suited to test our hypothesis because its plastic response is far from ideal plastic (see Fig. 1). This material displays a strong viscoplasticity and we selected a sample size such that deformation pattern is shearbanding, which results in a weakening before reaching the limit load (see Fig. 1). Moreover, the printing process influences the plastic properties of the resulting material [16]. It is therefore of great interest to select this material to test our approach, which eliminates the need for characterisation of the viscoplasticity and weakening law of the printed PLA. The method is first validated for a cylinder sample with the simplest microstructure, consisting of a single pore as Gurson studied. Then, we present an application of the method for a rock's microstructure, reconstructed from segmented μCT scan images.

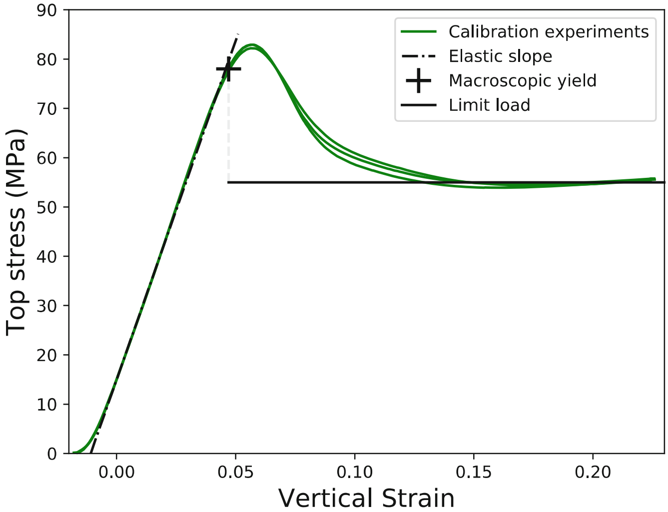

Fig. 1. Three stress strain curves of uniaxial compression of 3D printed full cylinders of PLA to observe the plastic response of the material and assess the reproducibility of mechanical tests on 3D printed samples. The proposed elasto-plastic model in this study is superposed to the curves and determined by three parameters: the slope of the linear elastic part, the macroscopic yield value, and the limit load (displayed on a wide range of strain for visualisation purposes).

2 Validation Against Analytical Yield Criterion

In this section, we verify that our hypothesis stating that the yield stress is mostly influenced by internal structure and not rheology stands for the simplest microstructure, a unique spherical pore. For this ideal structure, a yield criterion has already been derived semi-analytically by Gurson, as detailed in the introduction. Therefore, further simulations are only required in the following section for more complex structures.

The rheology considered is the one of the 3D printed PLA material displayed in Fig. 1. The polymer is known to be pressure insensitive which allows the uniaxial compression tests to characterise the limit load $q^{ref}{}_y$ of the material, found around 54 MPa. In order to 3D print the structure corresponding to Gurson's model, we simplify the geometry to 2D and the hollow sphere becomes a hollow cylinder with cylindrical hole which is easy to 3D print and the yield surface follows Gurson's criterion, expressed as

$$\frac{q_y}{q_y^{ref}}^2 = 1 + \phi^2 - 2\phi \cos h\left(\frac{3}{2}\frac{p_y}{q_y^{ref}}\right), \tag{1}$$

with p_y, q_y respectively the mean stress and Von Mises stress at yield and ϕ the porosity, equal to 0.25 in this study. The yield surface predicted by Gurson of the hollow cylinder of 3D printed PLA of height 48 mm and diameter 32 mm with a cylindrical hole of diameter 16 mm is plotted in Fig. 2.

FDM-based 3D printers are selected for this work, as they are one of the most popular consumer-level printers [2]. We used the Ultimaker 2+ printers available at the Shaping

Matter Lab of Delft University of Technology, which prints polymers composites based on the extrusion additive manufacturing (AM) system. Slicing parameters are selected such as to produce 3D printed samples of high quality and homogeneity which allows for the reproducibility of results as illustrated by the superposition of the stress-strain curves of Fig. 1. It is worth specifying that the infill density is set at 100% to keep the solid parts non-porous as the present study only considers porosity at a sample-scale level. The mechanical loading is done in uniaxial compression which gives one point of verification on the yield surface. A loading rate of 0.0016 mm/s is applied on the 3D printed hollow cylinder. In this section, we focus on the limit load since it corresponds to the state predicted by Gurson's yield criterion and the supplementary study on the macroscopic yield stress can be found in the study of Lesueur et al. [13]. The limit load is determined on the stress-strain curve similarly to Fig. 1. It is found at 39.1 Mpa, corresponding for a uniaxial compression stress path to a mean stress of 13.3 Mpa. This yield point falls exactly on the analytical yield surface as shown in Fig. 2, which proves that the yield stress for a simple structure can be approximated by an ideal elasto-plastic model.

3 Prediction of the Microstructure Influence on the Yield

The method is now tested against the complex microstructure of a real rock. The selected specimen is a cubic subsample of size 0.5 mm of the Berea sandstone [11].

Using the stack of segmented 2D μCT scan images, the geometry is meshed in 3D following the methodology described by Lesueur et al. [12]. In order to be processed by the Ultimaker machine for printing, the mesh is converted to an STL file format. The sample is printed as a cube of size 22 mm. The quality of the printed sample is quite remarkable as it captures very well the overall complexity of the original rock. Still, some details of the print remain imperfect, as can be seen in Fig. 3, due to the limit of the Fused Deposition Modelling printing technique for overhanging parts at an angle greater than 45º.

Five identically printed samples are then tested in uniaxial compression following the experimental procedure described in the previous section, with a loading speed of 0.08 mm/min. The resulting stress strain curves, plotted in Fig. 4a, resemble each other, that is, they share the same elastic properties and similar hardening tendencies but have noticeably different values of macroscopic yields. We can only infer that the lack of reproducibility is due to the insufficient printing resolution and quality because the curves of Fig. 1, whose samples' printing quality was high, superposed completely. Compared to Fig. 1, the curve of the sample shows no softening nor limit load, but instead hardens continuously. The complex pore network in the μCT scan results in a very disperse pore collapse over the whole sample (see plastic deformations in Fig. 2b) that could prevent therefore a homogeneous shearband from forming, which would explain the absence of softening.

In order to numerically determine the yield of this example, we simulate in Finite Element with REDBACK [17] the same uniaxial compression on a digital version of that same microstructure, reconstructed from μCT scans and meshed following the method of Lesueur et al. [12], with 796,636 structured elements. The boundary conditions applied

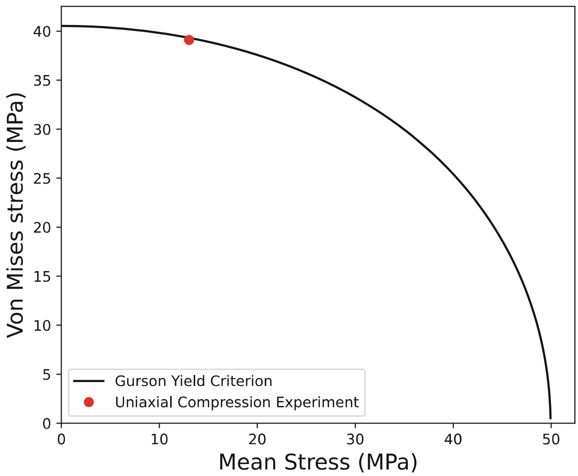

Fig. 2. Theoretical yield surface predicted by Gurson of the 3D printed hollow cylinder with a cylindrical hole. The red dot is the macroscopic yield point obtained from the unixial compression experiment on this specimen.

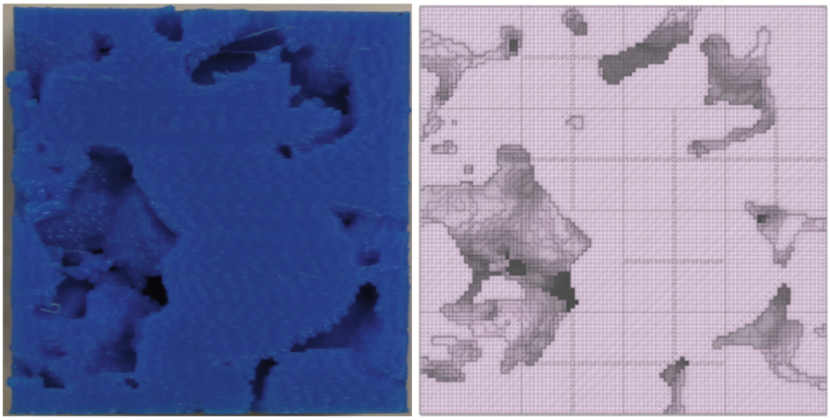

Fig. 3. Side face of the printed microstructure (a) compared to the digital rock (b).

are meant to reproduce a uniaxial compression and loaded with a prescribed strain rate. To retrieve exclusively the influence of the internal structure on the yield, we take an ideal *J2* model for the plasticity of the matrix material and calibrate this model to resemble the behaviour of the printed PLA. The resulting stress strain curve is plotted in Fig. 2a.

We note that for both numerical and experimental approach, we do not reach indeed a limit load as in Fig. 1. This confirms our interest in extending Gurson's exclusive study of the limit load to the macroscopic yield because the limit load does not exist for every material.

Despite that the match of Fig. 2a is not as impressive as that of Fig. 1 due to the precision loss on the 3D printing, the numerical and experimental curves still match qualitatively and display a similar shape. In this more complex example, the porous material appears to be stiffer and stronger (higher macroscopic yield) with the experimental approach. This could be explained by the reinforcement of the structure due to the existence of artificial bridges between pores that were created during the imperfect printing process. The suboptimal printing quality adds to the uncertainty of the experimental results, which brings us more confidence in the value of elasticity and macroscopic yield determined with the numerical approach.

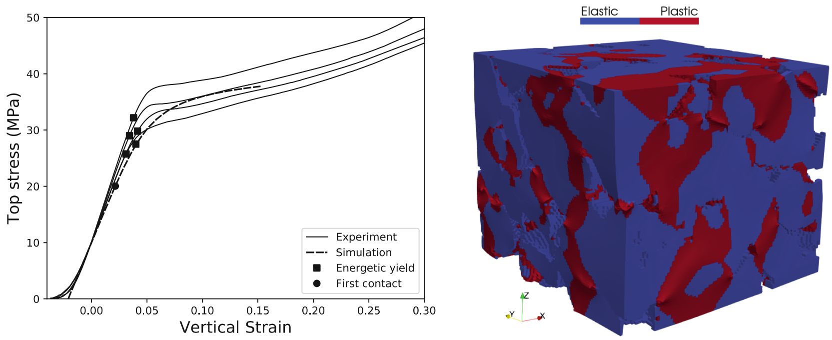

Fig. 4. (a) Experimental and numerical stress-strain curves of the uniaxial compression of 3D printed samples of the Berea sandstone [11]. (b) Visualisation of plastic deformations on the numerical uniaxial compression at 12% strain.

4 Conclusion

In this contribution, we presented an approach to determine the macroscopic yield of a porous material from finite element compression of its microstructure, replacing the traditional destructive testing approach. By focusing the study on the macroscopic yield instead of the complete mechanical behaviour, we have shown that the complex skeleton material can be satisfactorily approximated by an equivalent ideal elasto-plastic material before reaching the macroscopic yield. By reducing the complexity of the material implemented, simulations of mechanical compressions become more achievable.

References

1. Besson, J.: Damage of ductile materials deforming under multiple plastic or viscoplastic mechanisms. Int. J. Plast. **25**(11), 2204–2221 (2009)
2. Dizon, J.R.C., Espera Jr, A.H., Chen, Q., Advincula, R.C.: Mechanical characterization of 3D-printed polymers. Addit. manufact. **20**, 44–67 (2018)
3. Dunn, D.E., LaFountain, L.J., Jackson, R.E.: Porosity dependence and mechanism of brittle fracture in sandstones. J. Geophys. Res. **78**(14), 2403–2417 (1973)
4. Fritzen, F., Forest, S., Bohlke, T., Kondo, D., Kanit, T.: Computational homogenization of elasto-plastic porous metals. Int. J. Plast. **29**, 102–119 (2012)

5. Gologanu, M., Leblond, J.-B., Perrin, G., Devaux, J.: Recent extensions of gurson's model for porous ductile metals. In: Continuum Micromechanics, pp. 61–130. Springer Vienna, (1997)
6. Green, R.J.: A plasticity theory for porous solids. Int. J. Mech. Sci. **14**(4), 215–224 (1972)
7. Gurson, A.L.: Continuum theory of ductile rupture by void nucleation and growth: Part I—yield criteria and flow rules for porous ductile media. J. Eng. Mater. Technol. **99**(1), 2–15 (1977)
8. Hamiel, Y., Lyakhovsky, V., Agnon, A.: Coupled evolution of damage and porosity in poroelastic media: theory and applications to deformation of porous rocks. Geophys. J. Int. **156**(3), 701–713 (2004)
9. Hashin, Z., Shtrikman, S.: A variational approach to the theory of the elastic behaviour of multiphase materials. J. Mech. Phys. Solids **11**(2), 127–140 (1963)
10. Hoshino, K.: Effect of porosity on the strength of the clastic sedimentary rocks. In: Advances in rock mechanics: Proceedings of the 3rd Congress of International Society of Rock Mechanics, volume IIA, pp. 511–516, Denver, Colorado (1974)
11. Imperial College Consortium On Pore-Scale Modelling: Berea sandstone. (2014). https://doi.org/10.6084/m9.figshare.1153794
12. Lesueur, M., Casadiego, M.C., Veveakis, M., Poulet, T.: Modelling fluid-microstructure interaction on elasto-visco-plastic digital rocks. Geomech Energy Environ **12**, 1–13 (2017)
13. Lesueur, M., Poulet, T., Veveakis, M.: Predicting the yield strength of a 3d printed porous material from its internal geometry. Addit. Manuf. **44**, 102061 (2021)
14. Lesueur, M.: Influence of multiphysics couplings across scales: from digital rock physics to induced fault reactivation. PhD thesis, UNSW Sydney, School of Minerals and Energy Resources Engineering (2020)
15. Mackenzie, J.K.: The elastic constants of a solid containing spherical holes. Proceedings of the Physical Society. Section B **63**(1), 2–11 (1950)
16. Popescu, D., Zapciu, A., Amza, C., Baciu, F., Marinescu, R.: FDM process parameters influence over the mechanical properties of polymer specimens: a review. Polym. Test. **69**, 157–166 (2018)
17. Poulet, T., Paesold, M., Veveakis, M.: Multi-physics modelling of fault mechanics using redback: a parallel open-source simulator for tightly coupled problems. Rock Mech. Rock Eng. **50**(3), 733–749 (2017)
18. Springmann, M., Kuna, M.: Identification of material parameters of the gurson–tvergaard–needleman model by combined experimental and numerical techniques. Comput. Mater. Sci. **33**(4), 501–509 (2005)
19. Tvergaard, V.: Influence of voids on shear band instabilities under plane strain conditions. Int. J. Fract. **17**(4), 389–407 (1981)
20. Xie, S.Y., Shao, J.F.: Elastoplastic deformation of a porous rock and water interaction. Int. J. Plast. **22**(12), 2195–2225 (2006)